ChemComm

Accepted Manuscript

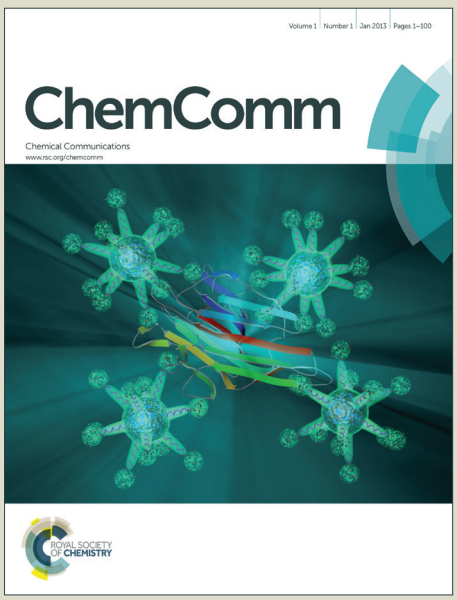

ROYAL SOCIETY OF CHEMISTRY

www.rsc.org/chemcomm

A Self-Assembled Nanotube for the Direct Aldol Reaction in Water

Kwang Soo Lee[a] and Jon R. Parquette*

The self-assembly of a low weight, dipeptide into well-defined nanotubes that catalyze the direct aldol reaction in water is reported.

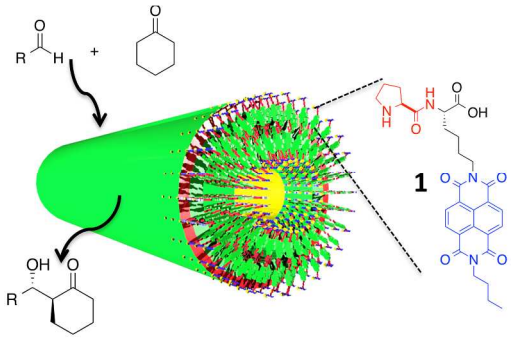

Chemical Communications

COMMUNICATION

A Self-Assembled Nanotube for the Direct Aldol Reaction in Water

Kwang Soo Lee[a] and Jon R. Parquette*[a,]

Received 00th January 20xx,
Accepted 00th January 20xx

DOI: 10.1039/x0xx00000x

www.rsc.org/

Nanotubes formed by the aqueous assembly of a proline-lysine dipeptide (1) were used to create the hydrophobic microenvironments required to catalyze the aldol reaction in water. The self-assembly process occurred most efficiently in the presence of the substrates, producing an array of homogeneous nanotubes under the reaction conditions. The nanotubes formed by dipeptide 1 served as an efficient catalyst for the aldol reaction that functioned at low loading levels and provided good to excellent conversions. The catalytic activity of 1 was minimal under conditions that dissociated the nanotube into soluble monomers.

Enzymes accelerate chemical reactions by folding into highly ordered structures that position reactants within microenvironments favorable for catalysis. There has been considerable interest in replicating this process using synthetic materials to create catalysts that operate efficiently in water.[1] Amphiphilic materials such as diblock polymers,[2-14] dendrimers,[15, 16] micelles,[17, 18] cyclodextrins[19, 20] and hydrogels[21] have been exploited to create local hydrophobic regions that promote reactions that normally fail in aqueous environments. These materials generally lack the internal structural order characteristic of enzymatic catalysts. Molecular self-assembly[22] offers an opportunity to expediently produce nanostructured materials comprised of simple subunits that are organized into highly ordered, tightly packed arrays.[23] The internal order within supramolecular nanofibers and nanopores[24] has been shown to provide enhanced hydrolytic properties, compared with solution-phase catalysts.[12, 25-27] Soft materials have more recently been developed to mediate photocatalytic water splitting,[28, 29] copper-catalyzed Diels Alder cycloadditions,[30] and metal-catalyzed processes.[31, 32]

L-Proline is well-known to catalyze the direct asymmetric aldol reaction between ketones and aldehydes with high efficiency and stereoselectivity in organic solvents, but proceeds poorly in water.[33] The reaction often proceeds in or "on" water when a separate hydrophobic microphase can be

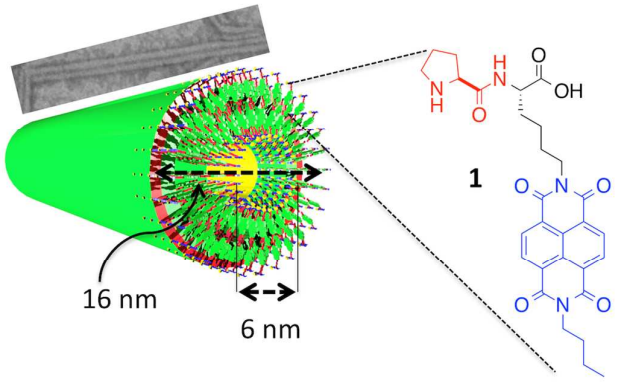

Figure 1. Self-assembly of Pro-Lys dipeptide **1** into nanotubes.

formed by a large excess of one of the reactants.[34] In these cases, the reaction presumably occurs within an organic phase, formed by the reactant, which sequesters the catalyst and reactants from the aqueous solvent. Strategies that isolate the organocatalytic site within a local hydrophobic pocket formed by the aggregation of amphiphilic peptides,[35] polymers,[17, 21, 36] dendrimers[37] or hydrophobically modified proline catalysts[38-41] enhance the efficiency of the process in water. The majority of these systems isolate the catalytic site within a hydrophobic pocket formed within a globular or, more rarely, a fibrillar nanostructure. Comparatively, nanotube 1-D assemblies offer greater surface-to-volume ratios, ready access to the interior via the open ends of the tube, and modular, highly uniform structural dimensions. However, the potential for nanotubes to serve as catalytic superstructures in water has not received significant attention.[32] Herein, we show that nanotubes formed via the β-sheet self-assembly of (L)-Pro-(L)-Lys dipeptide **1** catalyzes the direct aldol condensation in pure water at low catalyst loading levels (Fig. 1).

We previously described a strategy for the 1D self-assembly of dilysine peptides functionalized at the ε-amino

[a] Department of Chemistry and Biochemistry, The Ohio State University 151 W. Woodruff Ave., Columbus, OH 43210 (USA)

†Electronic Supplementary Information (ESI) available: synthetic produres, imaging and spectral characterization. See DOI: 10.1039/x0xx00000x

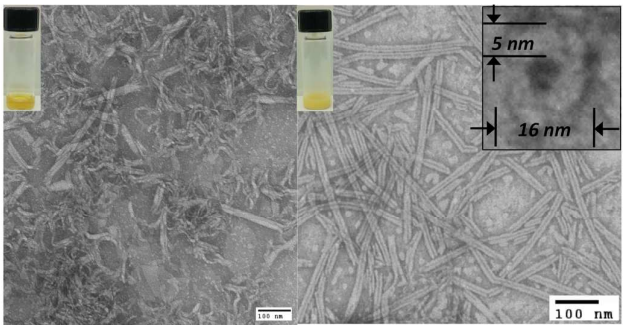

Figure 2. TEM images of dipeptide **1** dissolved in pure water (500 μM) (left) and in the reaction mixture containing 4-nitrobenzaldehyde and cyclohexanone in water (500 μM) (right). Inset: magnification of a protruding end of a nanotube. Samples were prepared by dissolving **1** in water (10 mM), prior to diluting to 500 μM and evaporating onto a carbon-coated copper grid with uranyl acetate as a negative stain.

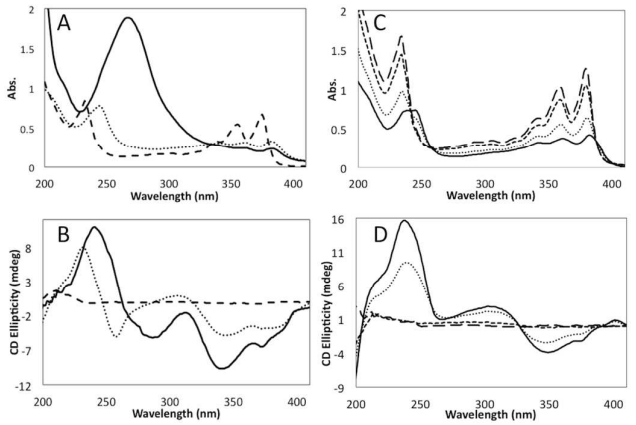

Figure 3. Left: (A) UV-Vis and (B) CD spectra of **1** (1 mM) in reaction mixture (solid), H_2O (dots) and TFE (dash). Right: (B) UV-Vis and (D) CD spectra of **1** in water with 10% (solid), 25% (dots), 50% (short dash) and 75% (long dash) TFE.

position on one residue with a 1,4,5,8-naphthalenetetracarboxylic acid diimide (NDI) chromophore.[42,43] Recently, this approach was exploited to create nanotubes functionalized with the anticancer drug, camptothecin.[44] Following this design strategy, we prepared a zwitterionic (L)-Pro-(L)-Lys dipeptide analog (**1**) containing a lysine, functionalized with an NDI on the side-chain, and a *N*-terminal proline residue (Fig. 1). This design would create nanotubes via the progressive helical winding of a β-sheet, bilayer assembly[45] that would position the catalytic proline residue, as part of the zwitterionic head group, along the inner and outer surface of the nanotube structure.

Dipeptide **1** was highly soluble in water, producing a translucent, light yellow solution at 10 mM. Transmission electron (TEM) micrographs of a sample prepared from a diluted solution of **1** (500 μM) revealed the presence of a mixture of nanofibers, helically twisted nanoribbons and nanotubes (Fig. 2, left). As shown in Figure 3a, the decreased intensity and red-shifting of NDI band I (350-400 nm) and band II (231 nm) UV-Vis absorptions, going from 2,2,2-trifluoroethanol (TFE) to water, are consistent with occurrence of *J*-type π-π interactions in the self-assembly of **1**.[46] The FTIR spectrum of **1** in D_2O exhibited a strong amide I ($\nu_{C=O}$) band at 1625 cm^{-1}, indicating that β-sheet structure (~78% by spectral deconvolution) stabilized the nanostructures (Fig. S3).[47-49] Similarly, the circular dichroism (CD) spectra revealed a flat line in TFE; whereas strongly negative excitonic Cotton effects corresponding to both π – π* absorption bands I and II of the NDI chromophore emerged in water (Fig. 3b). The negative chirality of these CD bands reflected an *M*-type helical, intermolecular packing orientation of the NDI rings within the nanostructures.[50]

Initial efforts to explore the capability of dipeptide **1** to catalyze the aldol reaction revealed that the addition of 4-nitrobenzaldehyde and cyclohexanone significantly impacted the self-assembly process. AFM and TEM images of the reaction mixture showed a uniform array of fully formed nanotubes with inner and outer diameters of ~16 and 6 nm, respectively (Fig. 2, right, Fig. S4). Comparison of the dimensions of the nanotube walls (~5.0 nm) and the fully extended structure of **1** (~2.5 nm) suggest a bilayer arrangement of the monomers. The amplitude of CD bands of **1** under the reaction conditions were generally increased, showing an apparent inversion in sign in the range of ~270-300 nm. The UV-Vis spectra featured a large, broad peak in this range (λ_{max} 268 nm), due to a π–π transition of 4-nitrobenzaldehyde. It is noteworthy that 4-nitrobenzaldehyde was not soluble in water in the absence of dipeptide **1**.

These observations suggest that the nanotubes formed by dipeptide **1** were capable of encapsulating substrates of the reaction. To explore this feature of the catalyst, we measured the amount of Nile Red that could be solubilized by the nanotubes in pure water and 50 mM NaCl solutions. Nile red is a neutral, polarity-sensitive probe that is insoluble in water and exhibits low fluorescence with a λ_{max} of 660 nm.[51] However, encapsulation of the dye within a hydrophobic microenvironment increases the emission intensity and induces a blue-shift.[52] Fluorescence spectra were recorded as solutions of **1** (10 mM, 0.2 μmol) in pure water and 50 mM NaCl were titrated with Nile Red (0.005 to 0.1 μmol) (Fig. S5). Emission maxima were observed at 607 and 609 nm in water and 50 mM NaCl, respectively, indicative of hydrophobic encapsulation of the dye within the nanotube structures. The encapsulation efficiencies were 6.8% for water and 12.5 mol% for 50 mM NaCl.

The catalytic activity of **1** for the aldol reaction of *p*-nitrobenzaldehyde with cyclohexanone was probed as a model reaction (Table 1). The reactions were performed in water with an aldehyde concentration of 100 mM and a 10-fold excess of ketone with varying catalyst loading levels. Using 10 mol% of **1**, 95% conversion was reached after ~96 h. The aldol product was obtained with 83.5% de (*anti*) and 79.7% ee. Lowering the catalyst loading to 1% provided a similar conversion after 120 h with slightly higher selectivities (Entries 1-6). The addition of 50 mM NaCl resulted in a slightly higher enantioselectivity, but

Table 1. Nanotube-catalyzed Aldol reaction.

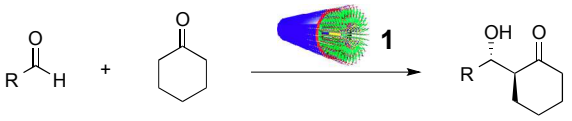

#	Cat.	R	Solv.[a]	Load (mol %)	Conv.[b] (%)	de_{anti}[c] (%)	ee_{anti}[d] (%)
1	**1**	4-$NO_2C_6H_4$	H_2O[f]	10	96	77.8	79.7
2	**1**	4-$NO_2C_6H_4$	H_2O	2.5	95	85.2	87.3
3	**1**	4-$NO_2C_6H_4$	H_2O[g]	2.5	82	85.2	91.9
4	**1**	4-$NO_2C_6H_4$	H_2O	1.0	91	86.9	88.0
5	**1**	4-$NO_2C_6H_4$	H_2O	0.5	76	88.7	81.0
6	**1**	4-$NO_2C_6H_4$	H_2O	0.25	52	86.9	79.7
7	**1**	4-$NO_2C_6H_4$	10% TFE-H_2O	10	86	84.7	78.6
8	**1**	4-$NO_2C_6H_4$	25% TFE-H_2O	10	51	84.3	75.4
9	**1**	4-$NO_2C_6H_4$	50% TFE-H_2O	10	trace	--	--
10	**1**	4-$NO_2C_6H_4$	75% TFE-H_2O	10	trace	--	--
11	**1**	4-$NO_2C_6H_4$	100% TFE	10	0	--	--
12	**1**	2-$NO_2C_6H_4$	H_2O	10	95	83.5	95.3
13	**1**	3-$NO_2C_6H_4$	H_2O	10	83	85.2	97.5
14	**1**	4-$MeO_2CC_6H_4$	H_2O	10	74	74.7	83.9
15	**1**	4-$CF_3C_6H_4$	H_2O	10	60	70.5	91.6
16	**1**		H_2O	10	11.6	40.0	43.0
17	**1**		H_2O, 50°C	10	97	55.6	45.5
18	**NBP**[e]	4-$NO_2C_6H_4$	H_2O	10	96	78.5	79.8
19	**NBP**	4-$NO_2C_6H_4$	H_2O	2.5	33	80.0	78.8
20	**NBP**	4-$NO_2C_6H_4$	H_2O	0.5	0	--	--

(a) Reactions were performed using aldehyde (1 equiv.), cyclohexanone (10 equiv.), catalyst and acetic acid (1 equiv. rel. to catalyst) at 25°C for 120 h, unless otherwise noted. (b) Conversion of aldehyde into aldol product, determined by ^{1}H NMR spectroscopy. (c) Determined by ^{1}H NMR spectroscopy. (d) Measured by HPLC on a chiral stationary phase (Daicel Chiralpak IA, 20% i-PrOH/hexane, UV 254 nm, Flow rate 1.0 mL/min). (e) NBP= *N*-benzyl prolinamide, 160 h. (f) 96 h (g) reaction run in presence of NaCl (50 mM).

slightly lower conversion. Although a decrease in the catalyst loading beyond 1% resulted in a progressive decrease in conversion, loadings as low as 0.25% produced 52% of the aldol product with similar selectivity. In contrast, using *N*-benzyl prolinamide as catalyst produced a biphasic solution that provided similar conversion and selectivities at 10 mol% after 160 h, but lower loading levels were much less effective, resulting in 0% conversion with 0.5 mol% catalyst.

Although other electron deficient groups at the 4-position of the aldehyde offered similar reactivites and selectivities, 2- and 3-nitrobenzaldehyde afforded significantly higher enantioselectivities (Entries 12-15). However, obtaining a reasonable reaction rate using cinnamaldehyde required elevating the temperature to 50°Ç, resulting in moderate enantioselectivity. It is noteworthy that the selectivity was only slightly diminished at 50°C, compared with ambient conditions (Entries 16-17).

To evaluate the impact of nanotube structure on the catalytic efficacy in water, the reaction was investigated as a function of the extent of self-assembly. As shown in Fig. 3c, the addition of TFE to aqueous solutions of **1** caused an increase in the amplitude and a blue-shift of the NDI absorption bands in the UV-Vis spectra, due to the progressive disassembly of the nanotubes with increasing TFE. Similarly, a progressive decrease in CD intensity was observed as TFE was added, resulting in a flat line at 50% TFE/water, due to the dissociated state of the catalyst under those conditions (Fig. 3d). Likewise, the degree of catalytic conversion decreased significantly as the ratio of TFE/water increased, exhibiting no activity above 50% TFE (Table 1, entries 7-11). These observations demonstrate the importance of self-assembly in creating local environments amenable for catalytic activity. The enantioselectivity was not significantly decreased in the presence of TFE, indicating that the isolated L-proline residue was primarily responsible for selectivity.

Table 2. Recyclability of **1** in reaction of 4-nitrobenzaldehyde with cyclohexanone.[a]

Cycle	Conv. (%)	d.e (%)	e.e (%)
1	96.1	77.8	85.3
2	92.5	76.2	87.5
3	91.0	76.0	90.1
4	86.5	74.3	92.6
5	83.6	72.6	93.5

(a) Recycling protocol: Each reaction cycle was performed as described in Table 1 at 25°C. After 120 h, the solution was extracted with CH_2Cl_2 to isolate the organic products, and the catalyst was removed by ultracentrifugation (80,000 rpm) of the water layer. The resultant catalyst pellet was used for the following reaction cycle.

In conclusion, we have shown that the self-assembly of a (L)-proline-(L)-lysine dipeptide (**1**) into nanotubes provides hydrophobic microenvironments capable of catalyzing the aldol reaction in water. The capability of the nanotubes to bind hydrophobic substrates was apparent in both the substrate-enhanced self-assembly process and by Nile Red binding experiments. The catalyst can be readily recovered by ultracentrifugation to sediment the nanotubes from the aqueous layer (Fig. S6). Although the conversion rate decreased slightly over five cycles, the selectivity improved from 85.3 to 93.5 % ee (Table 2). The enhanced selectivity and the associated decrease in conversion rate may be attributed to changes in the packing of **1** within the nanotubes over time Thus, the catalytic nanotubes offer a low weight, dipeptide precursor that operates at low loading levels and has potential for recovery/recycling via ultracentrifugation.

This work was supported by the National Science Foundation (CHE-1412295). We acknowledge the technical assistance and usage of the Campus Microscopy & Imaging Facility at OSU.

Notes and references

1. J. Meeuwissen and J. N. Reek, *Nat Chem*, 2010, **2**, 615-621.
2. R. K. O'Reilly, C. J. Hawker and K. L. Wooley, *Chem. Soc. Rev.*, 2006, **35**, 1068-1083.
3. I. A. Okhapkin, E. E. Makhaeva and A. R. Khokhlov, *Adv. Polym. Sci.*, 2006, **195**, 177-210.

4. M. Bortenschlager, N. Schollhorn, A. Wittmann and R. Weberskirch, *Chem. Eur. J.*, 2007, **13**, 520-528.
5. A. D. Ievins, X. F. Wang, A. O. Moughton, J. Skey and R. K. O'Reilly, *Macromolecules*, 2008, **41**, 2998-3006.
6. K. T. Kim, J. J. L. M. Cornelissen, R. J. M. Nolte and J. C. M. van Hest, *Adv Mater*, 2009, **21**, 2787-2791.
7. T. E. Kristensen, K. Vestli, K. A. Fredriksen, F. K. Hansen and T. Hansen, *Org. Lett.*, 2009, **11**, 2968-2971.
8. A. C. Evans, A. Lu, C. Ondeck, D. A. Longbottom and R. K. O'Reilly, *Macromolecules*, 2010, **43**, 6374-6380.
9. A. Laschewsky, J.-N. Marsat, K. Skrabania, H. von Berlepsch and C. Bottcher, *Macromol. Chem. Phys.*, 2010, **211**, 215-221.
10. A. Lu, T. P. Smart, T. H. Epps, 3rd, D. A. Longbottom and R. K. O'Reilly, *Macromolecules*, 2011, **44**, 7233-7241.
11. P. Cotanda, A. Lu, J. P. Patterson, N. Petzetakis and R. K. O'Reilly, *Macromolecules*, 2012, **45**, 2377-2384.
12. D. Zaramella, P. Scrimin and L. J. Prins, *J. Am. Chem. Soc.*, 2012, **134**, 8396-8399.
13. E. Huerta, P. J. Stals, E. W. Meijer and A. R. Palmans, *Angew. Chem. Int. Ed. Engl.*, 2013, **52**, 2906-2910.
14. I. K. Sagamanova, S. Sayalero, S. Martinez-Arranz, A. C. Albeniz and M. A. Pericas, *Catal. Sci. Technol.*, 2015, **5**, 754-764.
15. B. Helms, C. O. Liang, C. J. Hawker and J. M. J. Frechet, *Macromolecules*, 2005, **38**, 5411-5415.
16. C. O. Liang, B. Helms, C. J. Hawker and J. M. J. Frechet, *Chem. Commun.*, 2003, 2524-2525.
17. H. A. Zayas, A. Lu, D. Valade, F. Amir, Z. Jia, R. K. O'Reilly and M. J. Monteiro, *ACS Macro Letters*, 2013, **2**, 327-331.
18. S. Tascioglu, *Tetrahedron*, 1996, **52**, 11113-11152.
19. A. Uyanik, M. Bayrakci, S. Eymur and M. Yilmaz, *Tetrahedron*, 2014, **70**, 9307-9313.
20. K. Liu and G. Zhang, *Tetrahedron Lett.*, 2015, **56**, 243-246.
21. A. Lu, D. Moatsou, D. A. Longbottom and R. K. O'Reilly, *Chem. Sci.*, 2013, **4**, 965.
22. X. B. Zhao, F. Pan, H. Xu, M. Yaseen, H. H. Shan, C. A. E. Hauser, S. G. Zhang and J. R. Lu, *Chem. Soc. Rev.*, 2010, **39**, 3480-3498.
23. E. Busseron, Y. Ruff, E. Moulin and N. Giuseppone, *Nanoscale*, 2013, **5**, 7098-7140.
24. N. Sakai, N. Sorde and S. Matile, *J. Am. Chem. Soc.*, 2003, **125**, 7776-7777.
25. M. O. Guler and S. I. Stupp, *J. Am. Chem. Soc.*, 2007, **129**, 12082-12083.
26. C. Q. Zhang, X. D. Xue, Q. Luo, Y. W. Li, K. N. Yang, X. X. Zhuang, Y. G. Jiang, J. C. Zhang, J. Q. Liu, G. Z. Zou and X. J. Liang, *ACS Nano.*, 2014, **8**, 11715-11723.
27. Z. Huang, S. Guan, Y. Wang, G. Shi, L. Cao, Y. Gao, Z. Dong, J. Xu, Q. Luo and J. Liu, *J. Mater. Chem. B*, 2013, **1**, 2297.
28. V. Kunz, V. Stepanenko and F. Wurthner, *Chem. Commun.*, 2015, **51**, 290-293.
29. A. S. Weingarten, R. V. Kazantsev, L. C. Palmer, M. McClendon, A. R. Koltonow, A. P. Samuel, D. J. Kiebala, M. R. Wasielewski and S. I. Stupp, *Nat. Chem.*, 2014, **6**, 964-970.
30. Q. X. Jin, L. Zhang, H. Cao, T. Y. Wang, X. F. Zhu, J. Jiang and M. H. Liu, *Langmuir*, 2011, **27**, 13847-13853.
31. J. Potier, S. Menuel, M.-H. Chambrier, L. Burylo, J.-F. Blach, P. Woisel, E. Monflier and F. Hapiot, *ACS Catal.*, 2013, **3**, 1618-1621.
32. Z. Q. Li, Y. M. Zhang, Y. Chen and Y. Liu, *Chem. Eur. J.*, 2014, **20**, 8566-8570.
33. B. List, R. A. Lerner and C. F. Barbas, *J. Am. Chem. Soc.*, 2000, **122**, 2395-2396.
34. N. Mase and C. F. Barbas, 3rd, *Org. Biomol. Chem.*, 2010, **8**, 4043-4050.
35. J. Duschmale, S. Kohrt and H. Wennemers, *Chem. Commun.*, 2014, **50**, 8109-8112.
36. I. K. Sagamanova, S. Sayalero, S. Martínez-Arranz, A. C. Albéniz and M. A. Pericàs, *Catal. Sci. Technol.*, 2014, DOI: 10.1039/c4cy01344a.
37. Y. Y. Wu, Y. Z. Zhang, M. L. Yu, G. Zhao and S. W. Wang, *Org. Lett.*, 2006, **8**, 4417-4420.
38. F. Rodriguez-Llansola, J. F. Miravet and B. Escuder, *Chem. Commun.*, 2009, 7303-7305.
39. T. He, K. Li, M.-Y. Wu, M.-B. Wu, N. Wang, L. Pu and X.-Q. Yu, *Tetrahedron*, 2013, **69**, 5136-5143.
40. A. Patti and S. Pedotti, *Eur. J. Org. Chem.*, 2014, **2014**, 624-630.
41. L. Zhong, Q. Gao, J. B. Gao, J. L. Xiao and C. Li, *J. Catal.*, 2007, **250**, 360-364.
42. H. Shao, T. Nguyen, N. C. Romano, D. A. Modarelli and J. R. Parquette, *J. Am. Chem. Soc.*, 2009, **131**, 16374-16376.
43. H. Shao, J. W. Lockman and J. R. Parquette, *J. Am. Chem. Soc.*, 2007, **129**, 1884-1885.
44. S. H. Kim, J. A. Kaplan, Y. Sun, A. Shieh, H. L. Sun, C. M. Croce, M. W. Grinstaff and J. R. Parquette, *Chem. Eur. J.*, 2015, **21**, 101-105.
45. H. Shao, M. Gao, S. H. Kim, C. P. Jaroniec and J. R. Parquette, *Chem.-Eur. J*, 2011, **17**, 12882-12885.
46. B. A. Jones, A. Facchetti, M. R. Wasielewski and T. J. Marks, *Adv. Funct. Mater.*, 2008, **18**, 1329-1339.
47. Y. Cordeiro, J. Kraineva, M. P. B. Gomes, M. H. Lopes, V. R. Martins, L. M. T. R. Lima, D. Foguel, R. Winter and J. L. Silva, *Biophy. J.*, 2005, **89**, 2667-2676.
48. G. Zandomeneghi, M. R. H. Krebs, M. G. Mccammon and M. Fandrich, *Protein Sci.*, 2004, **13**, 3314-3321.
49. C. Toniolo and M. Palumbo, *Biopolymers*, 1977, **16**, 219-224.
50. J. Gawronski, M. Brzostowska, K. Kacprzak, H. Kolbon and P. Skowronek, *Chirality*, 2000, **12**, 263-268.
51. M. O. Guler, R. C. Claussen and S. I. Stupp, *J. Mater. Chem.*, 2005, **15**, 4507-4512.
52. A. P. Goodwin, J. L. Mynar, Y. Z. Ma, G. R. Fleming and J. M. J. Frechet, *J. Am. Chem. Soc.*, 2005, **127**, 9952-9953.